

Effect of repulsive finite-range Gaussian interaction on ground state properties of trapped rotating bosons

Mohd. Imran* and M. A. H. Ahsan†

Department of Physics, Jamia Millia Islamia (A Central University), New Delhi 110025, India

(Dated: August 25, 2021)

We use exact diagonalization to study a rotating system of $N = 2$ to 16 spinless bosons confined in quasi-two-dimensional harmonic trap and interacting via repulsive finite-range Gaussian potential with large s -wave scattering length. The diagonalization of the Hamiltonian matrix using Davidson algorithm, in subspaces of quantized total angular momenta L_z in slow rotating regime $0 \leq L_z \leq 2N$ is carried out to obtain the N -body lowest eigenenergy and eigenstate. To bring out the effect of quantum (Bose) statistics and consequent phase stiffness (rigidity) of the variationally obtained many-body wavefunction on various physical quantities, our study spans from few-body ($N = 2$) to many-body ($N = 16$) systems. Further, to examine the finite-range effect of the repulsive Gaussian potential on many-body ground state properties of the Bose-condensate, we obtain the lowest eigenstate, the critical angular velocity of single vortex state and the quantum correlation (measured) in terms of von Neumann entanglement entropy and degree of condensation. It is found that for small values of the range (measured by the parameter σ) of Gaussian potential, the ground state energy increases for few-boson ($2 \leq N \leq 8$) systems but decreases for many-boson ($N > 8$) systems. On the other hand for relatively large values of the range of Gaussian potential, the ground state energy exhibits a monotonic decrease, regardless of the number of bosons N . For a given N , there is found an optimal value of the range of Gaussian potential for which the first vortex (with $L_z = N$) nucleates at a lower value of the rotational angular velocity Ω_{c1} compared to the zero-range (δ -function) potential. Further, we observe that rotation and interactions are competing effects with former being dominant over the latter. With increase in the range of Gaussian potential, the value of von Neumann entropy decreases and the degree of condensation increases implying an enhanced quantum correlation and phase rigidity.

PACS numbers: 03.75.Hh, 05.30.Jp, 34.20.-b, 67.85.-d

I. INTRODUCTION

The experimental realization of Bose-Einstein condensation (BEC) at nanokelvin temperatures in alkali Bose atomic vapors [1–3] offers a possibility to examine the role of various energy scales (associated with size, zero-point motion, interaction, rotation etc.) in the physics of interacting bosons confined in a trap with an externally impressed rotation [4–7]. Contrary to existing bulk systems like liquid ^4He where several of these energy scales overlap, the new mesoscopic systems that provide decisive control (in the laboratory) over their physical parameters [8, 9] such as density, effective dimensionality and particle-particle interaction [10, 11], enables one to separate and study their effects on the quantum many-body states [12–14]. Further, with recent advances in BEC on optical lattices [15–17] and microchip traps [18, 19], few-body systems have become an experimental reality and attracted particular attention of theorists [20–26].

For dilute atomic gas systems at low-enough temperatures with short-ranged atom-atom interaction, the interparticle interaction is usually described by zero-range (δ -function) potential [5–7, 30–33]. This approach is useful in case of one dimensional systems as δ -function po-

tential is well understood and easy to handle in 1D. Unfortunately, such an interaction potential in 2D is not self-adjoint [30] and cannot be used in a manner analogous to its one dimensional counterpart. Using configuration interaction, it is shown in Ref. [34] that a δ -function potential is not suitable as a replacement for the two-body interaction in exact theories. Indeed a regularized 2D contact potential is analytically tractable [35] but harder to handle numerically. Further as the number of particles is increased beyond two, the complexity of the quantum states increases quickly and analytical treatment becomes intractable, leaving one only with a numerical recourse [31, 36]. It has been demonstrated that in order to tackle the limit of zero-range interaction numerically [37], a prohibitively large Hilbert space is required to obtain the many-body ground state. For numerical many-body simulation, one usually prefers a smooth, short-range, model interaction potential. This leads us to use the finite-range Gaussian potential as a model interparticle interaction [37–40], in the trapped boson system [41–43].

A better control over interparticle interaction, characterized by the strength and range of interaction, and being expandable within finite number of basis functions of the Hilbert space [37, 38], are few of the advantages of the Gaussian potential over the usual δ -function potential. Besides, most of the mean field as well as many-body calculations on harmonically confined interacting bosons with an externally impressed rotation have used

* alimran5ab@gmail.com

† mahsan@jmi.ac.in

only the lowest-Landau-levels (LLL), in which bosons occupy single-particle states with radial quantum number $n_r = 0$ and angular momentum quantum number m taking only positive sign. There has been several exact diagonalization studies [44, 45] wherein it has been argued that for slow rotating [46] and moderately to strongly interacting [47] bosons, it becomes necessary to consider the single-particle states beyond LLL approximation with $n_r = 0, 1, \dots$, while m is allowed to take positive as well as negative values in constructing the many-body basis states. We are thus motivated to study the many-body dynamics beyond LLL approximation in moderately interacting system with finite-range Gaussian potential.

In the present work, our aim is to investigate various quantum mechanical ground state properties of rotating system of N ($2 \leq N \leq 16$) spinless bosons interacting via finite-range repulsive Gaussian potential (of large s -wave scattering length) in a quasi-two-dimensional (quasi-2D) harmonic trap. The exact diagonalization of the many-body Hamiltonian matrix is carried out in given subspaces of quantized total angular momentum L_z using Davidson iterative algorithm [48] to obtain the lowest-energy eigenstates in the co-rotating frame. We focus on angular momentum regime $0 \leq L_z \leq 2N$ and are mainly interested in exploring the system in vicinity of single vortex ($L_z = N$) state. We examine the role of the range of interaction on various quantities of interest that are experimentally accessible such as the ground state energy, degree of condensation, von Neumann entanglement entropy and critical angular velocity Ω_{c1} of first vortex state $L_z = N$. The results obtained demonstrate that the use of repulsive interparticle Gaussian potential has significant effect on many-body ground state properties.

This paper is organized as follows. In Sec. II, we describe the model Hamiltonian of a rotating Bose system with finite-range Gaussian interaction in quasi-2D harmonic trap. We then introduce the single-particle reduced density matrix and the criterion for the existence of BEC, degree of condensation and von Neumann entanglement entropy. In Sec. III, we present our exact diagonalization results on a system of N bosons, to examine the finite-range effect of interaction on many-body ground state properties. We first examine the non-rotating system with $L_z = 0$ followed by the rotating system in different subspaces of $L_z > 0$ focusing on the first vortex state with $L_z = N$. Finally in Sec. IV, we summarize the main results of the present study.

II. THEORETICAL MODEL

A. The System and The Hamiltonian

We consider a system of N interacting spinless bosons each of mass M , trapped in a harmonic potential $V(\mathbf{r}) = \frac{1}{2}M(\omega_\perp^2 r_\perp^2 + \omega_z^2 z^2)$. The trap with x - y symmetry is taken to rotate about the z -axis with angular velocity

$\tilde{\Omega} \equiv \tilde{\Omega}\hat{e}_z$. Here $r_\perp = \sqrt{x^2 + y^2}$ is the radial distance of the particle from the trap center; ω_\perp and ω_z are the radial and the axial frequencies respectively, of the harmonic confinement. The axially symmetric trapping potential $V(\mathbf{r})$ is assumed to be highly anisotropic with $\lambda_z \equiv \omega_z/\omega_\perp \gg 1$, so that the many-body dynamics along z -axis is frozen. The confined system is thus effectively quasi-two-dimensional. We chose $\hbar\omega_\perp$ as the unit of energy and $a_\perp = \sqrt{\hbar/M\omega_\perp}$ the corresponding unit of length. Introducing $\Omega \equiv \tilde{\Omega}/\omega_\perp$ (≤ 1) as the dimensionless angular velocity and L_z (scaled by \hbar) the z projection of the total angular momentum operator, the many-body Hamiltonian in the co-rotating frame is given as $H^{rot} = H^{lab} - \Omega L_z$ where

$$H^{lab} = \sum_{j=1}^N \left[-\frac{1}{2}\nabla_j^2 + \frac{1}{2}\mathbf{r}_j^2 \right] + \frac{1}{2} \sum_{i \neq j}^N U(\mathbf{r}_i, \mathbf{r}_j) \quad (1)$$

The first two terms in the Hamiltonian (1) correspond to the kinetic and potential energies respectively. The third term $U(\mathbf{r}_i, \mathbf{r}_j)$, arises from the inter-particle interaction described by the normalized Gaussian potential [41–44]

$$U(\mathbf{r}_i, \mathbf{r}_j) = \frac{g_2}{2\pi\sigma^2} \exp \left[-\frac{(\mathbf{r}_i - \mathbf{r}_j)^2}{2\sigma^2} \right] \quad (2)$$

with parameter σ (scaled by a_\perp) being the effective range of the potential and the dimensionless parameter $g_2 \equiv 4\pi a_s/a_\perp$ is a measure of the strength of interaction where a_s is the s -wave scattering length taken to be positive ($a_s > 0$) so that the effective interaction is repulsive. In the limit $\sigma \rightarrow 0$, the normalized Gaussian potential in Eq. (2) reduces to the zero-range δ -function potential $g_2\delta(\mathbf{r} - \mathbf{r}')$ used in earlier studies [5]. In the opposite limit of $\sigma \rightarrow \infty$, the Gaussian potential $U(\mathbf{r}_i, \mathbf{r}_j) \rightarrow 0$ for given inter-particle separation $|\mathbf{r}_i - \mathbf{r}_j|$ and a given strength of interaction g_2 . The values of interaction range σ vary from zero to the system size $\sim a_\perp$. For a given value of σ , the s -wave scattering length in the parameter $g_2 = 4\pi a_s/a_\perp$ is adjusted in such a way that Na_s/a_\perp becomes relevant to the experimental value [5, 44]. In addition to being physically more realistic, the finite-range Gaussian potential (2) is expandable within a finite subspace of single-particle basis functions [49] and hence computationally more feasible [37, 38] compared to the zero-range δ -function potential [50].

Since the system being studied here is rotationally invariant in the x - y plane, the z -component of the total angular momentum is a good quantum number leading to block diagonalization of the Hamiltonian matrix in subspaces of L_z [44]. To obtain the many-body eigenstates, we carry out diagonalization of the Hamiltonian matrix in different subspaces of L_z with inclusion of lowest as well as higher Landau levels of the single-particle basis states in constructing the N -body basis states [43–45].

B. The single-particle basis states

The single-particle basis functions are chosen to be the eigenfunctions of the non-interacting single-particle Hamiltonian

$$H_{sp} = \frac{1}{2} (-\nabla_{\perp}^2 + r_{\perp}^2) - \Omega \ell_z + \frac{1}{2} (-\nabla_z^2 + \lambda_z^2 z^2), \quad (3)$$

identified as the harmonic oscillator Hamiltonian with an externally impressed rotation about the z -axis given the single-particle angular momentum ℓ_z . The eigensolutions of $H_{sp} u_{n,m,n_z}(\mathbf{r}) = \epsilon_{n,m,n_z} u_{n,m,n_z}(\mathbf{r})$, in dimensionless form, are known to be:

$$\begin{aligned} \epsilon_{n,m,n_z} &= (n+1-m\Omega) + \lambda_z (n_z + 1/2) \\ u_{n,m,n_z}(\mathbf{r}) &= \sqrt{\frac{(\frac{1}{2}\{n-|m|\})! \sqrt{\lambda_z/\pi^3}}{(\frac{1}{2}\{n+|m|\})! 2^{n_z} n_z!}} e^{-(r_{\perp}^2 + \lambda_z z^2)/2} \\ &\quad \times e^{im\phi} r_{\perp}^{|m|} L_{\frac{1}{2}(n-|m|)}^{|m|}(r_{\perp}^2) H_{n_z}(\lambda_z z^2) \end{aligned} \quad (4)$$

where $n = 2n_r + |m|$ with the radial quantum number $n_r = 0, 1, 2, \dots$ and the single-particle angular momentum quantum number $m = 0, \pm 1, \pm 2, \dots$. Here $L_{\frac{1}{2}(n-|m|)}^{|m|}(r_{\perp}^2)$ is the associated Laguerre polynomial and $H_{n_z}(\lambda_z z^2)$ the Hermite polynomial. With $\lambda_z \gg 1$, the system is taken to be quasi-2D and hence there is practically no excitation along the z -axis. We, therefore, set $n_z = 0$ in Eq. (4) implying that all the particles occupy the lowest-energy state $u_0(z) = (\lambda_z/\pi)^{1/4} e^{-\lambda_z z^2/2}$ of z co-ordinate degree of freedom, thereby reducing Eq. (4) to

$$\begin{aligned} \epsilon_{n,m} &= (n+1-m\Omega) + \lambda_z/2, \quad \text{with } n = 2n_r + |m| \\ u_{n,m}(\mathbf{r}) &= \sqrt{\frac{(\frac{1}{2}\{n-|m|\})! \sqrt{\lambda_z}}{(\frac{1}{2}\{n+|m|\})! \pi^3}} e^{-(r_{\perp}^2 + \lambda_z z^2)/2} \\ &\quad \times e^{im\phi} r_{\perp}^{|m|} L_{\frac{1}{2}(n-|m|)}^{|m|}(r_{\perp}^2). \end{aligned} \quad (5)$$

Restricting to $n_r = 0$ and taking $m \geq 0$ corresponds to the lowest-Landau level (LLL) approximation. Taking $n_r = 0, 1, 2, \dots$ and allowing m to take positive as well as negative values corresponds to going beyond LLLs [44, 45].

In the present work, we employ beyond LLL approximation by including the lowest as well as higher Landau levels of the single-particle basis states $u_{n,m}(\mathbf{r})$ with $n_r = \frac{1}{2}(n-|m|) = 0, 1$ and $m = 0, \pm 1, \pm 2, \pm 3, \dots$.

C. Construction of many-body basis states

The N -body basis states $\{\Phi_{\nu}(\mathbf{r}_1, \mathbf{r}_2, \dots, \mathbf{r}_N)\}$ in a given subspace of L_z are constructed as the symmetrized products of a finite number of single-particle basis functions $u_{n,m}(\mathbf{r})$ defined in Eq. (5). The many-body index

$\nu \equiv (\nu_0, \nu_1, \dots, \nu_{\mathbf{k}}, \dots, \nu_j)$ labeling the many-body basis function $\Phi_{\nu}(\mathbf{r}_1, \mathbf{r}_2, \dots, \mathbf{r}_N)$ stands for a set of single-particle quantum numbers $\{\mathbf{k} \equiv (n, m)\}$ and their respective occupancies $\{\nu_{\mathbf{k}}\}$. In the second-quantized notation, the Bose field operator is expanded in terms of single-particle basis functions as $\hat{\psi}(\mathbf{r}) = \sum_{\mathbf{k}} \hat{b}_{\mathbf{k}} u_{\mathbf{k}}(\mathbf{r})$ where $\hat{b}_{\mathbf{k}}(\hat{b}_{\mathbf{k}}^{\dagger})$ is the annihilation(creation) operator for the Bose quanta in state \mathbf{k} , obeying commutation rules. In occupation-number representation, the N -body basis function $|\Phi_{\nu}\rangle$ in a given subspace of L_z is written in second-quantized form as:

$$|\Phi_{\nu}\rangle \equiv \prod_{\mathbf{k}=0}^j \frac{1}{\sqrt{\nu_{\mathbf{k}}!}} (\hat{b}_{\mathbf{k}}^{\dagger})^{\nu_{\mathbf{k}}} |\text{vac}\rangle \equiv |\nu_0 \nu_1 \dots \nu_{\mathbf{k}} \dots \nu_j\rangle \quad (6)$$

with $\sum_{\mathbf{k}=0}^j \nu_{\mathbf{k}} = N$ and $\sum_{\mathbf{k}=0}^j m_{\mathbf{k}} \nu_{\mathbf{k}} = L_z$ where $\mathbf{k} = (n_{\mathbf{k}}, m_{\mathbf{k}})$. With these constraints on $\{\nu_{\mathbf{k}}, m_{\mathbf{k}}\}$, only the most relevant Fock states (spanning the active Fock space), constructed from the full single-particle basis set, are included.

D. Determination of variational many-body wavefunction

In Rayleigh-Ritz scheme [51] employed here, the N -body variational wavefunction $\Psi(\mathbf{r}_1, \mathbf{r}_2, \dots, \mathbf{r}_N)$ for a given N and L_z , is constructed as

$$\Psi(\mathbf{r}_1, \mathbf{r}_2, \dots, \mathbf{r}_N) = \sum_{\nu} C_{\nu} \Phi_{\nu}(\mathbf{r}_1, \mathbf{r}_2, \dots, \mathbf{r}_N) \quad (7)$$

where $\{C_{\nu}\}$ are the variational parameters to be determined. Having constructed the active Fock states as outlined in the previous subsection, we calculate the matrix elements and set up the eigenvalue problem $HC = EC$ where H is the Hamiltonian matrix and C is the column matrix formed by $\{C_{\nu}\}$. The eigenvalue problem is solved iteratively using Davidson algorithm [48] to determine the many-body ground and low-lying excited eigenstates.

For a system of N bosons confined in a harmonic trap rotating with angular velocity Ω , the thermodynamic equilibrium corresponds to minimizing the Helmholtz free energy $F(T, V, N) \equiv E(S, V, N) - TS$ given by $e^{-\beta F} = \text{Tr} [e^{-\beta(H^{lab} - \Omega L_z)}]$. At zero temperature, it reduces to $E = \langle \Psi_0 | (H^{lab} - \Omega L_z) | \Psi_0 \rangle$, where Ψ_0 is the variationally obtained ground state with total angular momentum L_z , in the non-rotating (laboratory) frame. Therefore, the many-body Hamiltonian H^{lab} in Eq. (1) is diagonalized in given subspaces of L_z to obtain the energy $E^{rot}(L_z, \Omega) = E^{lab}(L_z) - \Omega L_z$ in the co-rotating frame. This is equivalent to minimizing $E^{lab}(L_z)$ subject to the constraint that the system has angular momentum expectation value L_z with angular velocity Ω identified as the corresponding Lagrange multiplier.

E. Physical Quantities of Interest

Single-particle reduced density matrix (SPRDM). Starting from the normalized N -body ground state wavefunction $\Psi_0(\mathbf{r}_1, \mathbf{r}_2, \mathbf{r}_3, \dots, \mathbf{r}_N)$, obtained variationally through exact diagonalization; one can determine the zero-temperature single-particle reduced density matrix $\rho(\mathbf{r}, \mathbf{r}')$, by integrating out the degrees of freedom of $(N - 1)$ particles. Thus

$$\begin{aligned} \rho(\mathbf{r}, \mathbf{r}') &= \int \int \dots \int d\mathbf{r}_2 d\mathbf{r}_3 \dots d\mathbf{r}_N \\ &\times \Psi_0^*(\mathbf{r}, \mathbf{r}_2, \mathbf{r}_3, \dots, \mathbf{r}_N) \Psi_0(\mathbf{r}', \mathbf{r}_2, \mathbf{r}_3, \dots, \mathbf{r}_N) \\ &\equiv \sum_{\mathbf{n}, \mathbf{n}'} \rho_{\mathbf{n}, \mathbf{n}'} u_{\mathbf{n}}^*(\mathbf{r}) u_{\mathbf{n}'}(\mathbf{r}'). \end{aligned} \quad (8)$$

The above formulation is expressed in terms of single-particle basis functions $u_{\mathbf{n}}(\mathbf{r})$ with quantum number $\mathbf{n} \equiv (n, m)$. Being hermitian, it can be diagonalized to give

$$\rho(\mathbf{r}, \mathbf{r}') = \sum_{\mu} \lambda_{\mu} \chi_{\mu}^*(\mathbf{r}) \chi_{\mu}(\mathbf{r}'), \quad (9)$$

with normalization $\sum_{\mu} \lambda_{\mu} = 1$ and $\chi_{\mu}(\mathbf{r}) \equiv \sum_{\mathbf{n}} c_{\mathbf{n}}^{\mu} u_{\mathbf{n}}(\mathbf{r})$ where each μ defines a fraction of the BEC. The $\{\lambda_{\mu}\}$ are the eigenvalues, ordered as $1 \geq \lambda_1 \geq \lambda_2 \geq \dots \lambda_{\mu} \dots \geq 0$, and $\{\chi_{\mu}(\mathbf{r})\}$ are the corresponding eigenvectors of the single-particle reduced density matrix $\rho(\mathbf{r}, \mathbf{r}')$.

Von Neumann entanglement entropy. In order to measure the quantum correlation of a many-body ground state, we calculate von Neumann entanglement entropy [52–54] defined as

$$S_1 = -\text{Tr}(\hat{\rho}_1 \ln \hat{\rho}_1) \quad (10)$$

with $\hat{\rho}_1$ being the single-particle reduced density operator obtained from the many-body ground state wavefunction. In terms of eigenvalues $\{\lambda_{\mu}\}$ and eigenfunctions $\{\chi_{\mu}(\mathbf{r})\}$, then, the von Neumann entropy is evaluated explicitly as

$$S_1 = -\sum_{\mu} \lambda_{\mu} \ln \lambda_{\mu} \quad (11)$$

in subspaces of total angular momentum L_z . The entropy S_1 also provides information about the degree of condensation C_d . For instance, for a perfect BEC, the value of C_d approaches to unity correspondingly the value of S_1 is zero, from Eq. (12) and (11) respectively, since all bosons assume to occupy one and the same mode that is macroscopic eigenvalue $\lambda_1 \sim 1$ and $\lambda_{\mu} \sim 0$ for $\mu > 2$. As the condensate depletes (due to rotation or interaction), with more than one eigenvalue $\{\lambda_{\mu}\}$ becoming non-zero, S_1 increases and correspondingly C_d decreases.

Degree of condensation. It is to be noted that the usual definition of condensation for a macroscopic system, given by the largest eigenvalue λ_1 of the single-particle reduced density matrix Eq. (9), is not appropriate for systems with small number of particles being

studied here [41, 55]. For example, in the absence of condensation, there is no macroscopic occupation of a single quantum state and all eigenvalues of the single-particle reduced density matrix are of the same order, such a definition would imply a condensate though with small magnitude. To circumvent this situation, one introduces a quantity which is sensitive to the loss of macroscopic occupation called the degree of condensation defined as

$$C_d = \lambda_1 - \bar{\lambda} \quad (12)$$

where $\bar{\lambda} = \frac{1}{p-1} \sum_{\mu=2}^p \lambda_{\mu}$ is the mean of the rest of eigenvalues. It can be seen that the degree of condensation, defined as in Eq. (12), approaches zero for equal eigenvalues, as one would expect.

III. NUMERICAL RESULTS AND DISCUSSION

In the discussion below a system with $2 \leq N < 8$ bosons where the effect of quantum statistics is insignificant is referred to as few-boson system whereas a system with $N \geq 8$ bosons where the effect of quantum statistics begins to show up is referred to as many-boson system.

To be concrete, we consider an interacting system of $2 \leq N \leq 16$ Bose atoms of ^{87}Rb confined in an axially symmetric harmonic trap. The radial trapping frequency is taken to be $\omega_{\perp} = 2\pi \times 220$ Hz corresponding to the trap length $a_{\perp} = \sqrt{\hbar/M\omega_{\perp}} = 0.727 \mu\text{m}$ and the aspect ratio of the trap $\lambda_z \equiv \omega_z/\omega_{\perp} = \sqrt{8}$, so that the system has small extension $a_z = \sqrt{\hbar/M\omega_z} = a_{\perp} \lambda_z^{-1/2}$ in the z -direction and its dynamics along this axis can be assumed to be completely frozen resulting in a quasi-2D system. Recent advancements in atomic physics have made it possible to tune the strength of interaction (from weak to strong) in ultracold atomic vapors using Feshbach resonance [10, 11]. For the many-body system being studied here, the characteristic energy scale for the interaction is determined by the dimensionless parameter (Na_s/a_{\perp}) . Owing to increasing dimensionality of the Hilbert space with number of particles N , making computation impractical for N more than a few hundred particles. We in our calculation here vary the s-wave scattering length a_s to achieve suitable value of (Na_s/a_{\perp}) relevant to experimental situation [5]. In the results presented here, the parameters of Gaussian potential in Eq. (2) have been chosen as $0 \leq \sigma \leq 0.9$ (in units of a_{\perp}) and $a_s = 10000 a_0$ (where $a_0 = 0.05292$ nm is the Bohr radius) so that the parameter $(Na_s/a_{\perp}) \sim 1$ corresponds to moderate interaction [44, 45]. With this choice, the value of the dimensionless interaction parameter $g_2 = 4\pi a_s/a_{\perp}$ turns out to be 9.151. From now on, we fix the value of interaction parameter $g_2 = 9.151$ and vary the Gaussian range σ from zero (corresponding to δ -interaction limit) to a value determined by the system size $\sim a_{\perp}$. The N -body variational ground state wavefunction beyond lowest-Landau-level (LLL) approximation [44, 45] is obtained through exact diagonalization

of the Hamiltonian matrix for each of the subspaces of quantized total angular momentum $0 \leq L_z \leq 2N$ using Davidson iterative algorithm [48]. The results obtained with repulsive Gaussian interaction (2) allow us to study the effect of the range σ of interparticle interaction on various quantum mechanically interesting properties of the Bose-condensed gas discussed in the following.

A. Non-rotating System

When the system is subjected to external rotation with angular velocity $0 \leq \Omega < \Omega_{c1}$ (where Ω_{c1} is the critical angular velocity of the first vortex state), the total angular momentum state $L_z = 0$ corresponds to the many-body ground state (with lowest energy in the co-rotating frame). Here, we examine the non-rotating N -boson ($2 \leq N \leq 16$) ground state in $L_z = 0$ subspace as the range of interaction is varied over $0 \leq \sigma \leq 0.9$ for the repulsive Gaussian potential (2).

Many-body ground state energy. We first explore the dependence of N -body ground state energy on the parameter σ . In Fig. 1, we present the variation of ground state energy per particle (E/N) with the interaction range σ for $N = 2, 4, 8, 12$ and 16 bosons in $L_z = 0$ subspace. For $N = 2$ bosons, we observe in Fig. 1(a) that the ground state energy initially increases for small values of σ attaining a peak at $\sigma = 0.55$ and then decreases monotonically as σ is increased further. When the interaction range σ is much greater than the system size a_\perp (not shown in the figure), the ground state energy is found to approach the non-interacting value *i.e.* the interaction energy becomes negligible. Our results on σ -dependence of the ground state energy of $N = 2$ particle in small σ limit is in good agreement with a recent work [37].

To examine the effect of quantum statistics, we study N bosons with repulsive Gaussian potential (2) and find that there is a change in σ -dependence of the ground state energy as the number of bosons is increased. For few boson systems with $N \leq 4$, the effect of quantum statistics is insignificant and the results are qualitatively similar to those presented for $N = 2$ bosons. It is seen from Figs. 1(a) and 1(b) that the peak of the ground state energy per particle *versus* σ plot shifts to larger values of σ as the number of bosons is increased from $N = 2$ to $N = 4$. For $N = 8$, when the effect of quantum statistics begins to show up, the peak of the E/N *versus* σ plot shifts to smaller values of σ . This reversal in trend of the peak position of E/N *versus* σ plot is due to quantum statistics as N is increased from 2 to 8. For $N > 8$, the effect of quantum statistics becomes fully developed and the E/N *versus* σ plot exhibits a monotonic trend. Accordingly, we observe from Fig. 1(d) for $N = 12$ and Fig. 1(e) for $N = 16$ that the ground state energy changes very little for small values of σ but as σ is increased further over the range $0.1 < \sigma \leq 0.9$, the E/N *versus* σ plot exhibits a monotonic decrease showing no peak. The de-

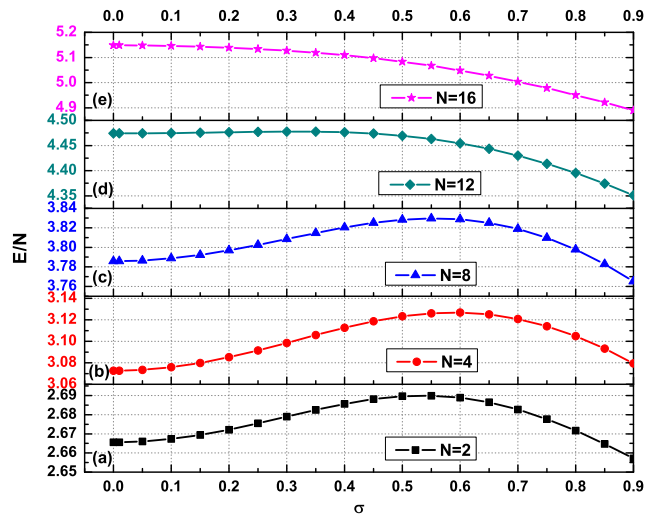


FIG. 1. (Color online) The non-rotating $L_z = 0$ state: ground state energy per particle E/N (in units of $\hbar\omega_\perp$) *versus* the interaction range σ (in units of a_\perp) of the Gaussian potential (2) with $g_2 = 9.151$ for a system of (a) $N = 2$ (b) $N = 4$ (c) $N = 8$ (d) $N = 12$ and (e) $N = 16$ bosons. The limiting case $\sigma \rightarrow 0$ corresponds to contact (δ -function) potential.

pendence of ground state energy on the interaction range σ is quite similar (always decreasing with increasing σ) for relatively large values of σ (< 1), regardless of the number of particles N . It, however, shows departure for small values of σ , namely, the ground state energy increases for small number of particles $2 \leq N \leq 8$ but remains constant for $N > 8$ as σ is increased.

Quantum correlation. To further analyze the effect of interaction range σ of the Gaussian potential (2) on the quantum mechanical correlation or phase coherence of the Bose-condensed gas, we calculate the single-particle reduced density matrix defined in Eq. (9). The many-body quantum correlation is measured, here, in terms of the von Neumann entanglement entropy S_1 and the degree of condensation C_d defined in Eq. (11) and Eq. (12), respectively.

We first examine the dependence of von Neumann entropy S_1 on the interaction range σ of the Gaussian potential (2). The results are presented in Fig. 2(a) where the values of entropy S_1 are plotted as a function of σ for a system of $N = 2, 4, 8, 12$ and 16 bosons in the angular momentum subspace $L_z = 0$. For a given N , the value of S_1 decreases with increase in σ and becomes linear at large values of σ (< 1). The dependence of S_1 on σ is qualitatively similar for all N -boson systems studied here. It is interesting to note that for relatively large particle numbers $N \geq 8$, the entropy S_1 decreases sharply with increasing σ as the quantum correlation increases with increasing N . Accordingly, S_1 *versus* σ plot for $N = 16$, the largest system considered in our case, is the steepest.

The above observation of many-body quantum correlation is further supported by our results on the degree

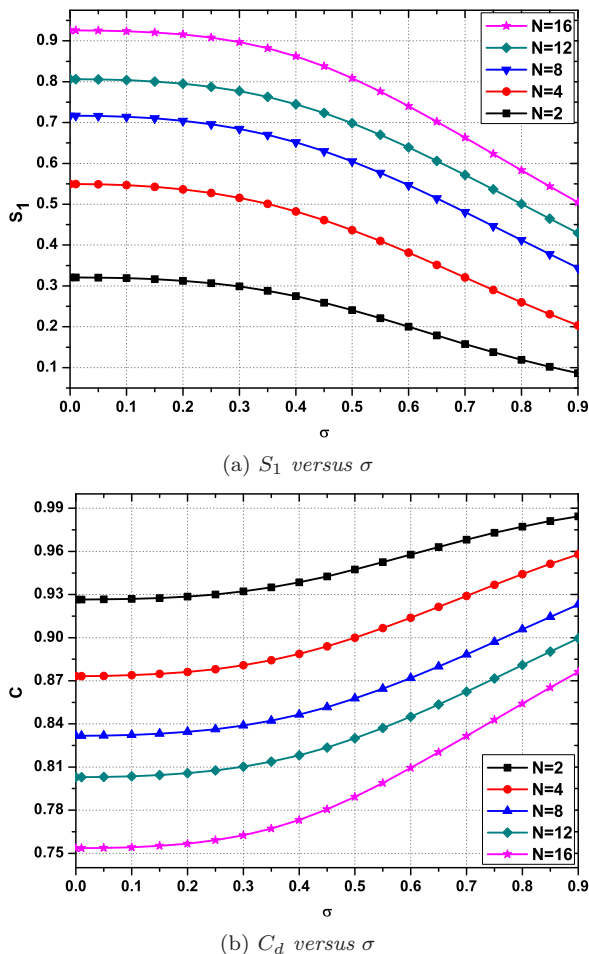


FIG. 2. (Color online) For the non-rotating system corresponding to $L_z = 0$ subspace, the N -body ground state of $N = 2$ (black squares), 4 (red circles), 8 (blue triangles), 12 (green rhombus) and 16 (pink stars) bosons interacting via Gaussian potential (2) with $g_2 = 9.151$; (a) von Neumann entropy S_1 and (b) degree of condensation C_d as a function of the interaction range σ (in units of a_\perp).

of condensation. In Fig. 2(b), we present degree of condensation C_d versus σ for a system of $N = 2, 4, 8, 12$ and 16 bosons. For a given N , it is seen from the figure, the value of C_d increases with increase in σ and the variation becomes linear for larger values of σ (< 1). Consequently, with increasing σ , the degree of condensation C_d increases and correspondingly von Neumann entropy S_1 decreases as shown in Fig. 2(a), leading to increase in quantum mechanical phase coherence. The explanation for such a behavior is that as the range σ of the Gaussian potential is increased, the broadened interparticle pair-potentials begin to overlap leading to increase in many-body effect. This increased many-body effect compared to the zero-range (δ -function) potential leads to an enhanced phase coherence, reflected in Figs. 2(a) and 2(b). Thus the finite-range (Gaussian) potential leads to Bose-Einstein condensate with relatively lower value of entropy and higher degree of condensation as compared to zero-

range (δ -function) potential [56].

We further observe from Fig. 2 that for a given value of σ , the von Neumann entropy S_1 gains a large value with increase in number of particles N , whereas, as a consequence of interparticle repulsion, the degree of condensation C_d decreases with increasing N i.e. the fragmentation is larger for larger number of Bosons N [25, 26]. A fragmented state is defined as a state for which there exists more than one macroscopically large eigenvalue of the SPRDM [27–29].

B. Rotating System

The results presented so far have been for the non-rotating $L_z = 0$ states. As the system is subjected to an external rotation, higher angular momentum states ($L_z > 0$) which minimize the free energy in the co-rotating frame, become the ground state [31]. We now examine the ground state properties of the rotating system as a function of the interaction range σ of the repulsive Gaussian potential in Eq. (2), for a fixed number of bosons N in different subspaces of quantized total angular momentum L_z . For the sake of comparison, the results are also presented for the non-rotating state $L_z = 0$ in the respective plots.

Many-body state energy. For a system of $N = 4$ and $N = 8$ bosons, Figures 3(a) and 3(b) respectively, present the variation of the lowest state energy per particle (E/N) in the co-rotating frame with the interaction range σ , in different subspaces of total angular momentum L_z . First, we consider a few-body system with $N = 4$ and observe from Fig. 3(a) that the σ -dependence of the lowest state energy per particle E/N corresponding to the state $L_z = 2$ is similar to the non-rotating ground state with $L_z = 0$. As the angular momentum is increased beyond $L_z = 2$, the energy per particle E/N increases, in general, linearly with σ . For small values of σ (< 0.1), the value of E/N does not change significantly with σ . However, for large values of σ (> 0.1), the effect of increasing rotation (increasing L_z) on E/N dominates over the effect of σ . When the particle number is increased to $N = 8$, the ground state energy E/N decreases with increasing σ for a given angular momentum ($L_z \neq 0$) and becomes almost linear for higher angular momentum states, as seen in Fig. 3(b). The trend is thus opposite to the one observed for $N = 4$ system and can be attributed to quantum (Bose-Einstein) statistics.

Quantum correlation. For a rotating system with a fixed number of bosons N , we calculate von Neumann entanglement entropy S_1 (11) and degree of condensation C_d (12), in different subspaces of total angular momentum L_z . In Fig. 4, we plot S_1 and C_d as a function of interaction range σ , for a few-boson system with $N = 4$ in subspaces $L_z = 0, 2, 4, 6, 8$. It is observed from Fig. 4(a) that for a given σ , the von Neumann entropy S_1 increases with increase in L_z . Further, in a given subspace of L_z , S_1 decreases for increasing σ specif-

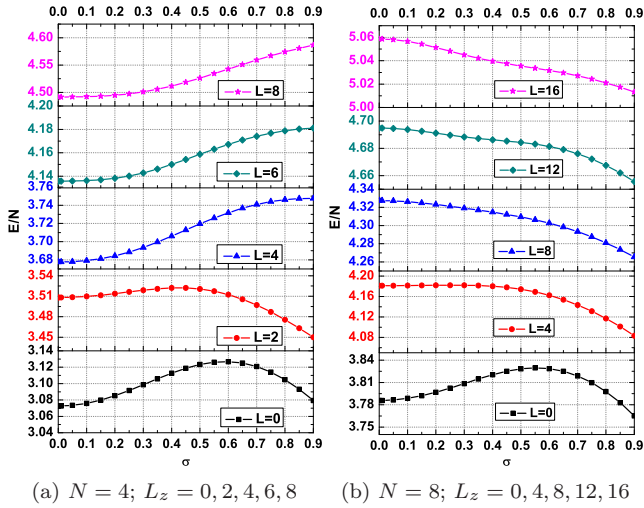


FIG. 3. (Color online) The ground state energy per particle E/N (in units of $\hbar\omega_{\perp}$) versus the interaction range σ (in units of a_{\perp}), in different subspaces of L_z , with interaction parameter $g_2 = 9.151$ of the Gaussian potential (2) for a rotating system of (a) $N = 4$ and (b) $N = 8$ bosons. The black line (squares) represents the ground state energy in $L_z = 0$ subspace of the respective non-rotating system, included here for reference.

ically at large values of σ . The decreasing behavior of S_1 with increasing σ , is relatively more pronounced for $L_z = 0, 2, 4, 8$ corresponding to no vortex, single vortex and two vortex states respectively, and moderate for the fragmented state $L_z = 6$, indicating thereby that the effect of rotation on S_1 is similar to the one observed with energy, as discussed above in Fig. 3(a) for $N = 4$ bosons. It is evident from Fig. 4(b) that the degree of condensation C_d increases gradually with increasing σ for a given L_z , except for the fragmented state $L_z = 6$, in which it is decreasing with increasing σ . Moreover, the curves C_d versus σ for the subspaces $L_z = 6$ and $L_z = 8$ intersect at $\sigma = 0.75$, implying the same value of degree of condensation. We find that over the range $0 \leq \sigma \leq 0.9$, the angular momentum state $L_z = 6$ is a fragmented state with more than one macroscopically large eigenvalues $\lambda_1 \sim \lambda_2$ of the SPRDM in Eq. (9). For example, at $\sigma = 0.75$ in $L_z = 6$ subspace for $N = 4$, the largest two eigenvalues of SPRDM are $\lambda_1 = 0.340$ and $\lambda_2 = 0.310$. On the other hand, at $\sigma = 0.75$ in $L_z = 8$ subspace corresponding to second vortex state for $N = 4$, the largest two eigenvalues of SPRDM are $\lambda_1 = 0.338$ and $\lambda_2 = 0.213$. In summary, the effect of interaction range σ and rotation are two competing effects; however, the effect of σ is overwhelmed by the effect of rotation since the energy scale of rotation *i.e.* $\hbar\Omega$ is large compared to the energy scale of interaction involving σ . Consequently, the effect of increasing σ in enhancing the quantum phase coherence (observed most pronounced in the non-rotating state with $L_z = 0$), is gradually destroyed by rotation with increasing L_z leading to the formation of fragmented state.

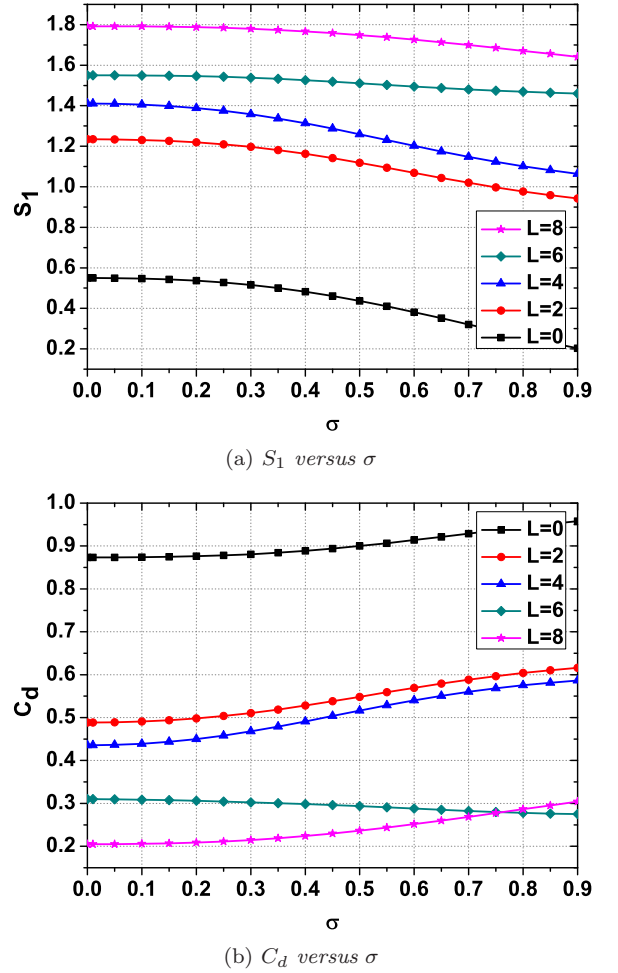


FIG. 4. (Color online) For a rotating system of $N = 4$ bosons in subspaces $L_z = 0$ (black squares), 2 (red circles), 4 (blue triangles), 6 (green rhombus) and 8 (pink stars), the variation of (a) von Neumann entropy S_1 and (b) degree of condensation C_d of the many-body quantum state, as a function of interaction range σ (in units of a_{\perp}) of the Gaussian potential (2) with interaction parameter $g_2 = 9.151$. The black line (squares) exhibit the results for the non-rotating system with $L_z = 0$, included here for reference.

We now consider a system of $N = 8$ bosons which appears to be large enough to exhibit the effect of quantum statistics leading to nucleation of first and second vortex states [58, 59]. We present in Fig. 5 the variation of von Neumann entropy S_1 and degree of condensation C_d with the interaction range σ , for $N = 8$ bosons in different subspaces of L_z . In Fig. 5(a), we observe that S_1 decreases with increasing value of σ in each subspace of L_z . This decreasing behavior of S_1 with σ is found to be steep for $L_z = 0, 8, 16$, moderate for $L_z = 4$ and approximately constant for $L_z = 12$. It is to be noted from the figure that for a given value of σ , the von Neumann entropy S_1 increases with increasing angular momenta L_z , except for the first vortex state. The value of S_1 is lower for the first vortex state with $L_z = N = 8$ compared to

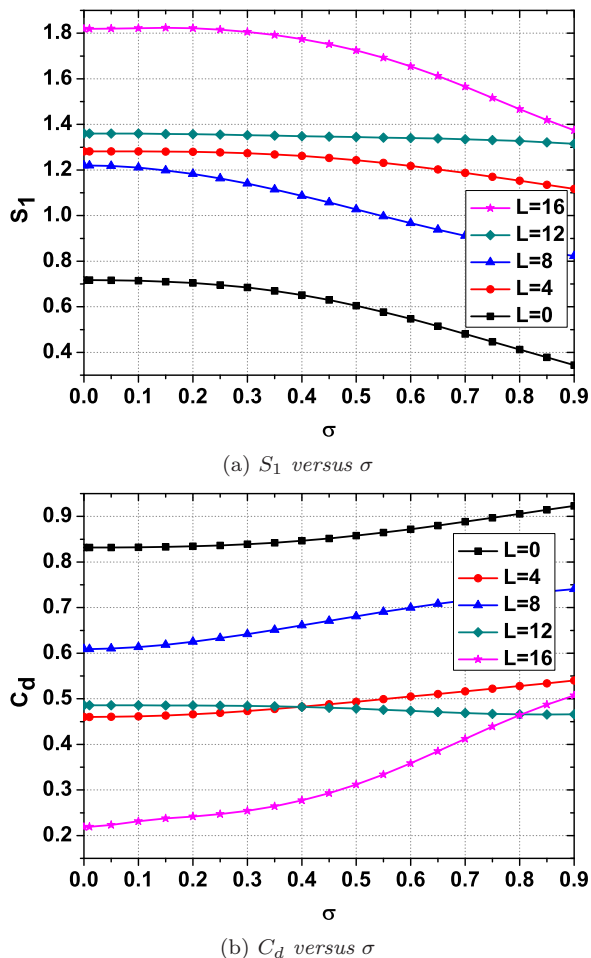


FIG. 5. (Color online) The variation of (a) von Neumann entropy S_1 and (b) degree of condensation C_d with interaction range σ (in units of a_\perp) of the Gaussian potential in Eq. (2) for a system of $N = 8$ bosons in subspaces of $L_z = 0$ (black squares), 4 (red circles), 8 (blue triangles), 12 (green rhombus) and 16 (pink stars); interaction parameter is chosen to be $g_2 = 9.151$. The black line (squares) exhibit the results for the non-rotating system with $L_z = 0$, included here for reference.

the state with $L_z = 4$. This is further supported by the fact that for a given σ , the degree of condensation C_d decreases with increasing L_z , except for the first vortex state $L_z = N = 8$ and the second vortex state $L_z = 12$, as seen in Fig. 5(b). Thus, for small values of $\sigma \leq 0.4$, the C_d versus σ curve for $L_z = 8$ and $L_z = 12$ vortical states shift to higher values of C_d compared to $L_z = 4$ state. However, for $L_z = 12$ state, we notice that the interaction range σ of the Gaussian potential has hardly any effect on S_1 and C_d . Further, the C_d versus σ curve for the second vortical state $L_z = 12$ intersects the C_d curves for $L_z = 4$ state at $\sigma = 0.4$ and $L_z = 16$ state at $\sigma = 0.8$. In the following subsection, we discuss the effect of σ on the critical angular velocity of the first vortex state with $L_z = N$.

C. First Vortex State

The non-rotating ground state of the system corresponds to total angular momentum $L_z = 0$. As the system is rotated, other (energetically favored) non-zero angular momentum states ($L_z \neq 0$) successively become the ground state of the system [31]. These are obtained by minimizing the energy in the co-rotating frame [44]

$$E^{rot}(\Omega, L_z, g_2) = E^{lab}(L_z, g_2) - \Omega L_z \quad (13)$$

where g_2 is the interaction parameter and Ω is the externally impressed angular velocity. The energy of a vortex-free state $E_0^{rot}(\Omega)$ in the rotating frame is numerically equal to the energy E_0^{lab} in the laboratory frame because the angular momentum of a vortex-free state is zero. A singly quantized vortex along the trap axis has total angular momentum $L_z = N$ [57, 58]; therefore, the corresponding energy of the system in the rotating frame is $E_1^{rot}(\Omega) = E_1^{lab} - \Omega N$. The difference between these two energies is

$$\Delta E^{rot}(\Omega) = E_1^{rot} - E_0^{rot} = E_1^{lab} - \Omega N - E_0^{lab}. \quad (14)$$

Setting $\Delta E^{rot}(\Omega)|_{\Omega_{c1}} = 0$ gives the critical angular velocity of the first vortex state with $L_z = N$,

$$\Omega_{c1} = \frac{E_1^{lab} - E_0^{lab}}{N} \quad (15)$$

expressed in terms of the energy E^{lab} of the Bose-condensed state with and without a vortex, obtained in the laboratory frame.

In Fig. 6, we plot the critical angular velocity Ω_{c1} of the first vortex state ($L_z = N$) as a function of the interaction range σ for a rotating system of $N = 4, 8, 12$ and 16 bosons. As is observed from the figure, for a given set of interaction parameters (g_2 and σ) of the repulsive Gaussian potential in Eq. (2), the critical angular velocity Ω_{c1} of the first vortex state ($L_z = N$) decreases with increase in number of bosons N [44]. It is further observed that as σ is increased, the critical angular velocity Ω_{c1} , decreases over a wide range of σ , regardless of the number of bosons N . Thus, for a rotating system of N bosons with a given interaction parameter g_2 , there is a value of σ for which the critical angular velocity Ω_{c1} takes a minimum value. This implies that for an optimal value of σ of the Gaussian potential, the nucleation of the first vortex may begin at a lower value of rotational angular velocity Ω as compared to the δ -function ($\sigma \rightarrow 0$) potential.

We notice from the figure that for small values of σ (< 0.1), there is little change in the value of critical angular velocity Ω_{c1} compared to its value for the δ -function potential ($\sigma \rightarrow 0$); as the value of σ is increased further, the change in Ω_{c1} becomes significant depending on the number of bosons N considered. For instance, as shown in Fig. 6(a) for $N = 4$ bosons, the critical angular velocity Ω_{c1} decreases for intermediate

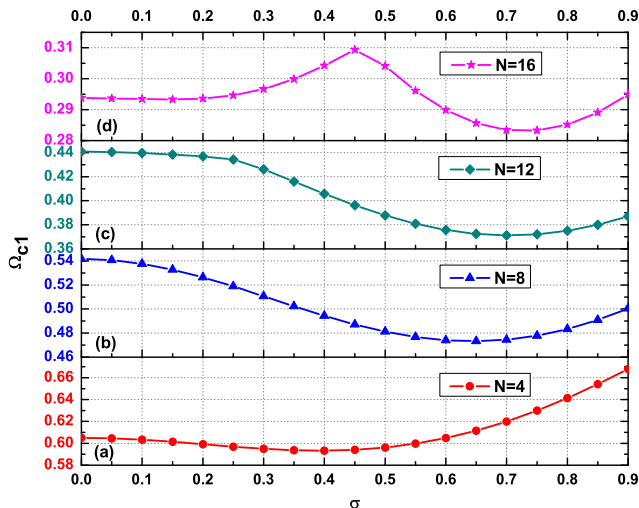


FIG. 6. (Color online) For N trapped bosons, critical angular velocity Ω_{c1} (in units of ω_{\perp}) of the first centered vortex state ($L_z = N$) versus the interaction range σ (in units of a_{\perp}) of the Gaussian potential (2). With fixed value of interaction parameter $g_2 = 9.151$, the minimum value of Ω_{c1} is observed (a) for $N = 4$ at $\sigma = 0.4$, (b) for $N = 8$ at $\sigma = 0.65$, (c) for $N = 12$ at $\sigma = 0.7$ and (d) for $N = 16$ at $\sigma = 0.75$ on the system size scale.

values of σ and then increases steeply for large values of σ . However, as seen in Fig. 6(b) for $N = 8$ (the least number of bosons in our present study where the effect of quantum statistics becomes significant), the decrease in value of Ω_{c1} with σ is steeper than for the $N = 4$ boson system. Similarly, beyond $\sigma = 0.25$, the decrease of Ω_{c1} with σ for $N = 12$ is steeper than for $N = 4$ as shown in Fig. 6(c). However, for $N = 16$ bosons shown in Fig. 6(d), Ω_{c1} increases initially with σ ; reaches a maxima at $\sigma = 0.45$ and then falls sharply with a minima at $\sigma = 0.75$. The different shape of Ω_{c1} versus σ curve for $N = 16$, compared to $N = 12, 8, 4$, can be attributed to quantum statistics. It is also observed that the critical angular velocity Ω_{c1} always increases for large values of $\sigma (< 1)$, regardless of the number of bosons N considered. Moreover, with increase in number of bosons, the minimum value of Ω_{c1} obtained with repulsive Gaussian potential shifts to larger values of σ .

In order to further support the above analysis of the single vortex state, we determine the difference in von Neumann entanglement entropy of the many-body state with and without a vortex, corresponding to the quantum mechanically stable states (in the co-rotating frame). For $N = 4, 8, 12$ and 16 bosons, Fig. 7 presents the finite-range effect of the Gaussian potential on the change in von Neumann entropy $\Delta S_1 = S_1(L_z = N) - S_1(L_z = 0)$ of the single vortex state with $L_z = N$ and the corresponding non-rotating state with $L_z = 0$. We observe a kink at $\sigma = 0.25$ and $\sigma = 0.45$ in the ΔS_1 versus σ plot for $N = 12$ and $N = 16$ bosons, respectively, which may be seen as a signature of an impending quantum phase

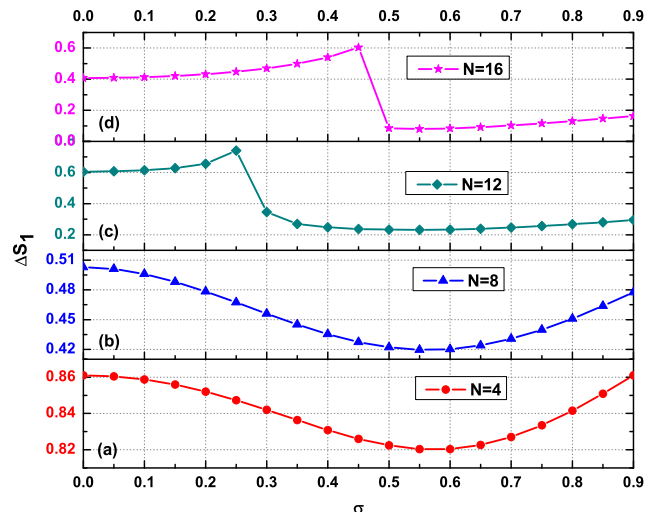


FIG. 7. (Color online) For N trapped bosons, change in entropy $\Delta S_1 = \{S_1(L_z = N) - S_1(L_z = 0)\}$ versus the interaction range σ (in units of a_{\perp}) with fixed value of interaction parameter $g_2 = 9.151$ of the Gaussian potential (2).

transition.

IV. SUMMARY AND CONCLUSION

In summary, we have presented an exact diagonalization study of the effect of repulsive Gaussian interaction with finite-range σ and large s -wave scattering length, on the rotating system of a finite number ($2 \leq N \leq 16$) of harmonically confined bosons in different subspaces of quantized total angular momentum L_z . The study considers variation with σ of several physical quantities (that are directly or indirectly accessible experimentally) such as lowest eigenstate energy, critical angular velocity (for nucleation of vortices) and quantum correlation (measured in terms of von Neumann entanglement entropy and degree of condensation) of the trapped Bose-condensed gas. The value of σ is varied over from zero (corresponding to δ -function interaction) to a value determined by the system size (measured in units of a_{\perp}). We explore the role of interaction range on the ground state properties of small systems ($N = 2$ to 8) where an understanding of few-body effect may provide valuable insight into large systems ($N = 8$ to 16) which admit the possibility of many-body correlation.

For the non-rotating ($L_z = 0$) system of $N = 2, 4, 8, 12, 16$ bosons, the variation of ground state energy with interaction range σ is analyzed. It is found that for small values of σ , the ground state energy increases for few-boson ($2 \leq N \leq 8$) system but decreases for many-boson ($N > 8$) system. On the other hand for relatively large values of $\sigma (< 1)$, the ground state energy exhibits a monotonic decrease, regardless of the number of bosons N , with the system reducing to a droplet of

bosons [22] where quantum statistics ceases to play any significant role. Further, for a given N , with increasing σ , the value of von Neumann entropy decreases and the degree of condensation increases. Thus, one achieves a more phase-rigid Bose-Einstein condensate with relatively lower value of entropy and higher degree of condensation using repulsive finite-range Gaussian potential compared to zero-range (δ -function) potential.

For a rotating system in the angular momentum regime $0 \leq L_z \leq 2N$, it is observed that the effect of rotation (with quantized L_z for a given N) competes with the effect of interaction range σ on the ground state properties of the Bose-condensate, though the former effect dominates over the latter effect. In a given subspace of $L_z (> 0)$, the value of lowest energy with σ increases gradually for few boson system ($N = 4$) but decreases for a system like $N = 8$ where the quantum statistics begins to show up. This observation supports the notion that when the particle number is increased to $N = 8$, the σ -dependence of the energy follows a trend opposite to that of $N = 4$ and can be attributed to quantum (Bose-Einstein) statistics. For a given L_z , the quantum correlation is enhanced with increasing σ (similar to the non-rotating $L_z = 0$ state) as the von Neumann entropy decreases and degree of condensation increases, specifically at large values of σ . However, for a given σ , the von Neumann entropy increases and degree of condensation decreases with increase in L_z *i.e.* rotation.

We further observe that for a given interaction range σ , the critical angular velocity Ω_{c1} of the single vortex state ($L_z = N$) decrease with increase in number of bosons N [44]. However, an increase in σ leads, in general, to a smaller critical angular velocity Ω_{c1} regardless, of the number of bosons N . For a given number N of bosons, there is a value of σ for which the critical angular velocity Ω_{c1} attains a minimum value indicating that there is an optimal value of σ of the Gaussian potential for which the nucleation of the first vortex begins at a lower value of rotational angular velocity compared to the zero-range δ -function potential. With increase in number of bosons N , the minimum value of Ω_{c1} obtained with Gaussian potential shifts to larger values of σ .

Thus, we find that in a quasi-2D system, the effect of interaction range of the repulsive Gaussian potential on the ground state properties is negligible for small values of $\sigma (< 0.1)$. However, the effect becomes significant for values of σ over the range $1 > \sigma > 0.1$) on the system size scale a_{\perp} . The results of the present study demonstrates the suitability of finite-range Gaussian interaction as a model for two-body interaction in a quantum many-body Bose system. With the possibility of experimental realization of few-body quantum system and the experimental controllability of the interatomic interaction via Feshbach resonance, the present theoretical work on dilute atomic vapors will be useful for the study of rotating quantum many-body systems with more realistic interaction potential in two dimensions.

-
- [1] M. H. Anderson, J. R. Ensher, M. R. Matthews, C. E. Wieman and E. A. Cornell, *Science*, **269**, 198 (1995).
- [2] K. B. Davis, M.-O. Mewes, M. R. Andrews, N. J. van Druten, D. S. Durfee, D. M. Kurn and W. Ketterle, *Phys. Rev. Lett.* **75**, 3969 (1995).
- [3] C. C. Bradley, C. A. Sackett, J. J. Tollett and R. G. Hulet, *Phys. Rev. Lett.* **75**, 1687 (1995).
- [4] See, Proceedings of the International School of Physics “Enrico Fermi”, Course CXL, 1999, edited by M. Inguscio, S. Stringari, and C. E. Wieman (IOS Press, Netherlands, 1999).
- [5] F. Dalfovo, S. Giorgini, L. P. Pitaevskii, and S. Stringari, *Rev. Mod. Phys.* **71**, 463 (1999).
- [6] A. L. Fetter and A. A. Svidzinsky, *J. Phys.-Cond. Matt.* **13**, R135 (2001).
- [7] A. J. Leggett, *Rev. Mod. Phys.* **73**, 307 (2001).
- [8] C. J. Pethick and H. Smith, *Bose-Einstein Condensation in Dilute Gases*, (Cambridge University Press, Cambridge, England, 2002).
- [9] J. F. Annett, *Superconductivity, superfluids and condensates*, (Oxford University Press, Bristol, 2003).
- [10] S. Inouye, M. R. Andrews, J. Stenger, H.-J. Miesner, D. M. Stamper-Kurn, and W. Ketterle, *Nature* **392**, 151 (1998).
- [11] C. Chin, R. Grimm, P. Julienne, and E. Tiesinga, *Rev. Mod. Phys.* **82**, 1225 (2010).
- [12] I. Bloch, J. Dalibard and W. Zwerger, *Rev. Mod. Phys.* **80**, 885 (2008).
- [13] N. R. Cooper, *Adv. Phys.* **57**, 539 (2008).
- [14] A. L. Fetter, *Rev. Mod. Phys.* **81**, 647 (2009).
- [15] O. Morsch and M. Oberthaler, *Rev. Mod. Phys.* **78**, 179 (2006).
- [16] W. S. Bakr, A. Peng, M. E. Tai, R. Ma, J. Simon, J. I. Gillen, S. Fölling, L. Pollet, and M. Greiner, *Science* **329**, 547 (2010).
- [17] J. F. Sherson, C. Weitenberg, M. Endres, M. Cheneau, I. Bloch, and S. Khur, *Nature (London)* **467**, 68 (2010).
- [18] R. Long, T. Steinmetz, P. Hommelhoff, W. Hänsel, T. W. Hänsch, and J. Reichel, *Philos. Trans. R. Soc. London, Ser. A* **361**, 1375 (2003).
- [19] J. Fortágh and C. Zimmermann, *Rev. Mod. Phys.* **79**, 235 (2007).
- [20] C. Yannouleas and U. Landman, *Rep. Prog. Phys.* **70**, 2067 (2007).
- [21] S. Viefers, *J. Phys.-Cond. Matt.* **20**, 123202 (2008).
- [22] H. Saarikoski, S. Reimann, A. Harju, and M. Manninen, *Rev. Mod. Phys.* **82**, 2785 (2010).
- [23] R. Islam, R. Ma, P. M. Preiss, M. E. Tai, A. Lukin, M. Rispoli, and M. Greiner, *Nature (London)* **528**, 77 (2015).
- [24] D. Blume, *Rep. Prog. Phys.* **75**, 046401 (2012).
- [25] Pere Mujal, Enric Sarlé and Artur Polls and Bruno Juliá-Díaz, *Phys. Rev. A* **96**, 043614 (2017).
- [26] G.C. Katsimiga, S.I. Mistakidis, G.M. Koutentakis, P. G. Kevrekidis, P. Schmelcher, *New J. Phys.* **19**, 123012 (2017).

- [27] O. Penrose and L. Onsager, Phys. Rev. **104**, 576 (1956).
- [28] P. Nozieres and D. Saint James, J. Phys. (Paris) **43**, 1133 (1982).
- [29] E. J. Mueller, T.-L. Ho, M. Ueda, and G. Baym, Phys. Rev. A **74**, 033612 (2006).
- [30] T. Busch, B.-G. Englert, K. Rzaewski, and M. Wilkens, Found. Phys. **28**, 549 (1998).
- [31] N. K. Wilkin and J. M. F. Gunn, Phys. Rev. Lett. **84**, 6 (2000).
- [32] N. R. Cooper, N. K. Wilkin, and J. M. F. Gunn, Phys. Rev. Lett. **87**, 120405 (2001).
- [33] X.-J. Liu, H. Hu, and P. D. Drummond, Phys. Rev. B **82**, 054524 (2010).
- [34] B. D. Esry and C. H. Greene, Phys. Rev. A **60**, 1451 (1999).
- [35] A. Farrell and B. P. van Zyl, J. Phys. A **43**, 015302 (2010).
- [36] G. F. Bertsch and T. Papenbrock, Phys. Rev. Lett. **83**, 5412 (1999).
- [37] R. A. Doganov, S. Klaiman, O. E. Alon, A. I. Streltsov and L. S. Cederbaum, Phys. Rev. A, **87**, 033631 (2013).
- [38] J. Christensson, C. Forssén, S. Åberg and S. M. Reimann, Phys. Rev. A **79**, 012707 (2009).
- [39] S. Klaiman, A. U. J. Lode, A. I. Streltsov, L. S. Cederbaum, and O. E. Alon, Phys. Rev. A **90**, 043620 (2014).
- [40] Peter Jeszenszki, Alexander Yu. Cherny and Joachim Brand, Phys. Rev. A **97**, 042708 (2018).
- [41] Mohd. Imran and M. A. H. Ahsan, Adv. Sci. Lett. **21**, 2764 (2015).
- [42] Mohd. Imran and M. A. H. Ahsan, Commun. Theor. Phys. **65**, 473 (2016).
- [43] Mohd. Imran and M. A. H. Ahsan, J. Phys. B: At. Mol. Opt. Phys. **50**, 045301 (2017).
- [44] M. A. H. Ahsan and N. Kumar, Phys. Rev. A **64**, 013608 (2001).
- [45] X.-J. Liu, H. Hu, L. Chang and S.-Q. Li, Phys. Rev. A **64**, 035601 (2001).
- [46] With rotational angular velocity much less than the trapping frequency, the degeneracy of the Landau levels is lifted even without interparticle interaction.
- [47] The particle-particle interaction causes different single-particle angular momentum states to scatter into each other.
- [48] E. R. Davidson, J. Comput. Phys., **17**, 87 (1975).
- [49] K. Huang, *Statistical Mechanics* (John Wiley & Sons, New York, 1987).
- [50] The exact diagonalization of the Hamiltonian matrix for finite N -body problem yields an exact variational solution within the basis chosen. For reasons of computational feasibility, it becomes necessary to truncate the set of single-particle basis functions used in the construction of many-body variational wavefunction. The δ -function potential $g_2\delta(\mathbf{r}-\mathbf{r}') = g_2\sum_{\mathbf{n}}u_{\mathbf{n}}^*(\mathbf{r})u_{\mathbf{n}}(\mathbf{r}')$, where summation \mathbf{n} runs over all basis states, is expandable in an infinite set of single-particle basis and hence computationally not suitable for exact diagonalization [49].
- [51] E. K. U. Gross, L. N. Oliveira and W. Kohn, Phys. Rev. A **37**, 2805 (1988).
- [52] R. Paškauskas, and L. You, Phys. Rev. A **64**, 042310 (2001).
- [53] Z. Liu, H. Guo, S. Chen, and H. Fan, Phys. Rev. A **80**, 063606 (2009).
- [54] Z. Liu and H. Fan, Phys. Rev. A **81**, 062302 (2010).
- [55] D. Dagnino, N. Barberà, K. Osterloh, A. Riera, and M. Lewenstein, Phys. Rev. A **76**, 013625 (2007).
- [56] J. Y. Lee, X. W. Guan, A. del Campo, and M. T. Batchelor, Phys. Rev. A **85**, 013629 (2012).
- [57] K. W. Madison, F. Chevy, W. Wohlleben, and J. Dalibard, Phys. Rev. Lett. **84**, 806 (2000).
- [58] D. A. Butts and D. S. Rokhsar, Nature (London) **397**, 327 (1999).
- [59] G. M. Kavoulakis, B. Mottelson, and C. Pethick, Phys. Rev. A **62**, 063605 (2000).